

Nucleosynthesis in Fast Expansions of High-Entropy, Proton Rich Matter

G. C. Jordan IV and B. S. Meyer

*Department of Physics and Astronomy, Clemson University, Clemson, SC 29634-0978,
USA*

gjordan@clemson.edu

ABSTRACT

We demonstrate that nucleosynthesis in rapid, high-entropy expansions of proton-rich matter from high temperature and density can result in a wider variety of abundance patterns than heretofore appreciated. In particular, such expansions can produce iron-group nuclides, p-process nuclei, or even heavy, neutron-rich isotopes. Such diversity arises because the nucleosynthesis enters a little explored regime in which the free nucleons are not in equilibrium with the abundant ^4He . This allows nuclei significantly heavier than iron to form in the presence of abundant free nucleons early in the expansion. As the temperature drops, nucleons increasingly assemble into ^4He and heavier nuclei. If the assembly is efficient, the resulting depletion of free neutrons allows disintegration flows to drive nuclei back down to iron and nickel. If this assembly is inefficient, then the large abundance of free nucleons prevents the disintegration flows and leaves a distribution of heavy nuclei after reaction freezeout. For cases in between, an intermediate abundance distribution, enriched in p-process isotopes, is frozen out. These last expansions may contribute to the solar system's supply of the p-process nuclides if mildly proton-rich, high-entropy matter is ejected from proto-neutron stars winds or other astrophysical sites. Also significant is the fact that, because the nucleosynthesis is primary, the signature of this nucleosynthesis may be evident in metal poor stars.

1. Introduction

Apart from numerous important studies of explosive hydrogen burning in matter accreted onto white dwarfs or neutron stars and early attempts to understand the p-process nuclei in terms of hydrogen burning in supernovae (Burbidge et al. 1957; Audouze & Truran

1975), astrophysicists have focused relatively little attention on explosive nucleosynthesis in proton-rich stellar environments. There are two principal reasons for this. First, after hydrogen burning, mainline stellar evolution proceeds at conditions of equal numbers of neutrons and protons, or, because of weak interactions, at a slight degree of neutron richness. Accordingly, if the star subsequently explodes, the resulting nucleosynthesis typically occurs in a neutron-rich environment. Only if the exploding matter has not finished hydrogen burning will the nucleosynthesis typically be proton-rich and proceed in a series of proton capture and β^+ -decay reactions known as the rp-process (Wallace & Woosley 1981). Such nucleosynthesis occurs when matter accreted onto the surfaces of white dwarfs or neutron stars explodes under degenerate conditions, giving rise to novae or X-ray bursts.

The second reason is that the nucleosynthesis is thought to be already relatively well understood. The details of the rp-process have been well-studied (e.g, Schatz et al. 2001) since it was first delineated. For proton-rich matter that achieves higher temperatures, it is generally imagined that the proton-rich nucleosynthesis would freezeout from an equilibrium in which iron-group isotopes would dominate the abundances. The underlying equilibrium abundance distribution might be slightly modified by proton captures at the end of the burning.

The purpose of this letter is to show that explosive nucleosynthesis in proton-rich environments can be much more complex than previously thought. While it is indeed the case that the final abundances for many conditions are dominated by iron-group isotopes, for sufficiently fast, high-entropy expansions of proton-rich matter, isotopes considerably heavier than iron can form. These other distributions of nuclei can include interesting quantities of light and heavy p-process isotopes or even neutron-rich species usually ascribed to the r-process.

We have not identified an astrophysical site in which such fast, high-entropy, proton-rich expansions may occur. The setting envisioned, however, is a neutrino-driven wind from a high-mass proto-neutron star early in its epoch of Kelvin-Helmholtz cooling by neutrino emission. Some calculations find wind entropies s/k_B of order 100–200 and expansion timescales (which we here define as the radial expansion timescale, $\tau = r/v$, where r is the radial coordinate and v is the radial velocity of a parcel of wind matter) as short as a few milliseconds (e.g, Thompson et al. 2001). The Y_e , that is, the electron-to-baryon ratio, in these winds is set by the interaction of neutrinos and antineutrinos with free nucleons. While the antineutrino spectrum from the neutron star is considerably harder than the neutrino spectrum at late times, which tends to make the wind neutron rich, it is possible that the two spectra are more nearly equal earlier. This could allow for proton-rich (that is, $Y_e > 0.5$) matter since the lower mass of the proton would favor the reaction $\nu_e + n \rightarrow p + e^-$ over the

reaction $\bar{\nu}_e + p \rightarrow n + e^+$.

2. Calculations

The model of the expansion of matter occurring in the fast winds is based on the previous fast expansion calculations of Meyer (2002) and similarly uses the Clemson Nucleosynthesis Code (Meyer 1995) with NACRE (Angulo et al. 1999) and NON-SMOKER (Rauscher & Thielemann 2000) rate compilations. In these calculations, material expands at constant entropy from high temperature and density. In the present parameterization, a fluid element in the wind moves out homologously so that its velocity $v \propto r$, and r grows exponentially in time with timescale τ . This means the density declines exponentially with time on a timescale $\tau/3$. This approximates the acceleration phase of the wind (e.g., Qian & Woosley 1996).

We computed several fast expansions. The final overproductions are presented in Table 1. For all calculations, the initial composition of the starting material was a mixture of protons and neutrons which gave the desired initial value of Y_e . This material was given an initial temperature of $T_9 = T/10^9 \text{ K} = 10.0$ and an initial density consistent with the chosen value of entropy. The calculations were halted after the temperature had dropped below $T_9 = 0.01$, by which time all capture reactions had long since ceased and nuclei were only beta-decaying back to stability. The values of τ , s , and initial Y_e are used when referencing specific calculations.

We first focus on a particularly interesting expansion with $s/k_B = 145$, $\tau = 0.003$ seconds, and $Y_e = 0.510$, which produces a significant quantity of the light p-process nuclei ^{94}Mo and ^{96}Ru . Figure 1 shows the nuclear abundances as a function of atomic number for four times in the expansion. A significant abundance of remarkably high-mass nuclei builds up early in the expansion. This surprising result arises from the fact that the abundances of the light nuclei ^2H , ^3H , and ^3He are low at high entropies. As a result, nuclear flows assembling ^4He , which proceed through these light nuclei, become too slow to maintain an equilibrium between the free nucleons and ^4He . As the temperature falls, equilibrium between the free nucleons and ^4He would increasingly drive the free nucleons to assemble into ^4He ; however, the slowness of the requisite reaction flows prevent this from occurring at the necessary rate. Though this equilibrium fails early (by $T_9 \approx 9$), the system is still primarily composed of ^4He . For this particular calculation, at $T_9 \approx 6$ the system is roughly 90% ^4He , 6% protons and 4% neutrons by mass with only a slight dusting of heavy nuclei. By $T_9 \approx 5$ the system is roughly 95% ^4He , 3.5% protons, and 1.5% neutrons by mass. From $T_9 = 6$ to $T_9 = 5$, the number of heavy nuclei have increased from $\sim 10^{-8}$ to 10^{-6} per

nucleon; thus, the heavy nuclei are still negligible in abundance compared to the protons, neutrons, and ${}^4\text{He}$. The critical point is that the disequilibrium between free nucleons and ${}^4\text{He}$ allows a large abundance of free nucleons to exist at temperatures that would normally see the free nucleons locked into ${}^4\text{He}$. The few heavy nuclei that have been forming at these times thus coexist with a large overabundance of free nucleons (Meyer 2002). Through a rapid sequence of neutron and proton captures these few heavy nuclei are driven to quite high nuclear mass, as shown in the $T_9 = 4.39$ panel in Figure 1. The peak at $Z \approx 58$ arises from the fact that the nuclear flows dam up at the closed neutron shell at $N = 82$.

As the temperature continues to fall, new heavy nuclei assemble from the abundant ${}^4\text{He}$ nuclei. The growing abundance of heavy nuclei is then increasingly able to catalyze the synthesis of ${}^4\text{He}$ from free neutrons and protons through reaction cycles such as ${}^{56}\text{Ni}(n,\gamma){}^{57}\text{Ni}(n,\gamma){}^{58}\text{Ni}(p,\gamma){}^{59}\text{Cu}(p,\alpha){}^{56}\text{Ni}$. Once the neutrons disappear (which helped hold the nuclear abundances at the higher mass, nonequilibrium distribution), the heavy nuclei begin to disintegrate towards iron-group nuclei, the favored isotopes in the equilibrium appropriate at those conditions. The $T_9 = 3.93$ panel of Figure 1 shows the abundance distribution shortly after this disintegration flow begins. The peak at $Z = 50$ arises from the fact that at this point the nuclear flow is damming up at the $Z = 50$ closed shell. By $T_9 = 3.80$, the disintegration flow has broken through $Z = 50$ and is now dammed up at $N = 50$, and predominantly at the isotope ${}^{92}\text{Mo}$. As the temperature continues to decline, proton captures deplete ${}^{92}\text{Mo}$ and create a large abundance of ${}^{94}\text{Ru}$ and ${}^{96}\text{Pd}$. These isotopes subsequently decay to ${}^{94}\text{Mo}$ and ${}^{96}\text{Ru}$ after reaction freezeout.

It is essential to note the large final abundances of protons and ${}^4\text{He}$. These species, and even a residual quantity of neutrons, are abundant throughout the disintegration epoch. This high abundance of neutrons, protons, and ${}^4\text{He}$ nuclei hinders the disintegrations, despite the high temperatures at the time the disintegrations are occurring ($T_9 \approx 4$). As mentioned above, the high abundance of protons also leads to proton-capture reactions along the $N = 50$ closed shell that modify the abundances at late times.

Table 1 presents top ten overproduction values from six calculations of nucleosynthesis in fast, high-entropy, proton-rich expansions. Calculation (B) is the model discussed above ($s = 145 k_B$, $Y_e = 0.510$, and $\tau = 0.003$ seconds). As discussed above, the most overproduced isotopes are light p-nuclei, which are made as $N = 50$ progenitors. At the top of the list are ${}^{96}\text{Ru}$ (made as ${}^{96}\text{Pd}$) and ${}^{94}\text{Mo}$ (made as ${}^{94}\text{Ru}$) at overproduction factors of $\sim 10^6$. Also significantly produced are ${}^{95}\text{Mo}$ (made as ${}^{95}\text{Rh}$) and ${}^{92}\text{Mo}$, which, although depleted late in the expansion by proton captures, is ultimately produced off of the $N=50$ shell as ${}^{92}\text{Ru}$.

Calculations (A) and (F) show results for expansions with lower entropy ($s = 140 k_B$) or lower Y_e ($Y_e = 0.505$) than in our reference calculation, (B). In both cases, the disintegration

flow began earlier in the expansion than in calculation (B) and allowed the nuclei to return to the iron-group isotopes before freezeout. On the other hand, the larger entropy in calculation (C) delayed the onset of disintegration and thereby strongly overproduced higher-mass p-process isotopes. In calculation (D), still heavier proton-rich isotopes formed. Rare isotopes such as ^{180}Ta are particularly strongly produced in this expansion. Finally, in calculation (E), the entropy was sufficiently high that the neutrons disappeared only at low temperature so the disintegration flow never occurred. This proton-rich expansion was able to produce heavy, neutron-rich isotopes whose production is normally associated with rapid neutron capture nucleosynthesis (cf. Meyer 2002). These results show the remarkable sensitivity of the nucleosynthesis to small changes in the expansion parameters.

Because of this sensitivity and the non-equilibrium aspect of the nuclear flows during key epochs of the expansion, we expect that, for a given set of expansion parameters, the nucleosynthetic yields of such proton-rich expansions will be particularly sensitive to nuclear reaction rates on a large suite of isotopes. This is confirmed in Table 2, which show results for calculations identical to calculation (C) but with all charged-particle and electromagnetic rates on nuclei with $Z \geq 27$ increased or decreased by a factor of two. In the former case, the larger reaction cross sections enhance the assembly of nucleons into ^4He and cause earlier and more efficient disintegration of the heavy isotopes into iron-group nuclei. In the latter case, the assembly of nucleons and, hence, the disintegration flows are less efficient and a heavier distribution of nuclei results than in calculation (C). Reaction surveys will be needed to further clarify this issue.

3. Implications

As Table 1 shows, there is a considerable variety of final abundance yields arising in these expansions. We do not expect these fast, proton-rich expansions to be dominant contributors to the solar system’s r-process isotopes: the overproductions are low and the final abundance pattern is different from the solar system’s r-process pattern. On the other hand, these expansions can make interesting quantities of rare isotopes (such as ^{180}Ta) and p-process nuclei, perhaps most intriguingly, the light p-process isotopes.

The precise mechanism for the production of the light p-process nuclei, $^{92,94}\text{Mo}$ and $^{96,98}\text{Ru}$, remains mysterious. While the heavier p-process isotopes are well accounted for by the “gamma-process” in either core-collapse supernovae (Woosley & Howard 1978) or perhaps in thermonuclear explosions (Howard et al. 1991), the same nucleosynthesis underproduces the light p-isotopes. This is because, unlike the heavy p-process nuclei, the light p-process isotopes are nearly as abundant as their r-process and s-process counterparts, which serve as

seeds for the gamma-process. This suggests some other process than the “gamma-process” may be responsible for their origin (although questions remain about the need for an exotic site (Costa et al. 2000)). Suggested other sites or processes are thermonuclear supernovae (Howard et al. 1991), alpha-rich freezeouts in core-collapse supernovae (Fuller & Meyer 1995; Hoffman et al. 1996), or the rp-process (e.g., Schatz et al. 2001). Each of these processes or sites has its own difficulties in either producing the right isotopes or actually ejecting them into interstellar space, and the question of the site of origin of the light p-process nuclei remains.

As evident from Table 1, the typical overproduction factors for calculations that produce light p-process isotopes are $\sim 10^6$. Core-collapse supernovae are responsible for production of ^{16}O , and such supernovae typically overproduce this isotope by a factor of about 10 (e.g., Woosley & Weaver 1995). If we assume light p-isotopes are 1) produced in rapid, high-entropy, proton-rich expansions in all core-collapse supernovae, 2) are overproduced at a level of $\sim 10^6$, and 3) are diluted into $10 M_{\odot}$ of ejecta, then we find each supernova must eject $\sim 10^{-4} M_{\odot}$ of this high-entropy, proton-rich matter. This is comparable to the estimates of the total mass ejected in proto-neutron star winds (e.g., Thompson et al. 2001); therefore, such winds may contribute interesting amounts of light p-process nuclei to the solar system if they indeed eject mildly proton-rich matter with the right timescales and entropies. On the other hand, some other as yet uncharacterized astrophysical site may achieve the necessary conditions. A full mapping of parameter space is clearly needed to understand this nucleosynthesis process as well as an exploration of its possible astrophysical settings.

Because winds from proto-neutron stars may evolve from slightly proton rich to neutron rich with time, p-process and r-process nucleosynthesis may occur in the same site with the former preceding the latter by a few tenths of a second, the timescale on which the neutrino and antineutrino spectra are changing. This may have interesting implications for the coupling or decoupling of r-process and p-process isotopes in cosmochemical samples (e.g., Yin et al. 2002).

Finally, we note that comparison of observations of abundances of Sr, Y, and Zr in low-metallicity stars and models of the chemical evolution of the Galaxy hint at a “lighter element primary process” (LEPP) that may contribute to the synthesis of $A \approx 90$ nuclei (Travaglio et al. 2004). The process we describe is primary and could therefore be an interesting component of this inferred LEPP.

The authors are grateful to D. D. Clayton, M. D. Leising, and J. R. King for discussions and to L.-S. The for assistance. This work was supported by NSF grant AST 98-19877,

NASA grant NAG5-10454, and a grant from DOE's SciDAC programs.

REFERENCES

- Angulo, C., Arnould, M., Rayet, M., Descouvemont, P., Baye, D., Leclercq-Willain, C., Coc, A., Barhoumi, S., Aguer, P., Rolfs, C., Kunz, R., Hammer, J. W., Mayer, A., Paradellis, T., Kossionides, S., Chronidou, C., Spyrou, K., degl'Innocenti, S., Fiorentini, G., Ricci, B., Zavatarelli, S., Providencia, C., Wolters, H., Soares, J., Grama, C., Rahighi, J., Shotter, A., & Laméhi Rachti, M. 1999, *Nuclear Physics A*, 656, 3
- Audouze, J. & Truran, J. W. 1975, *ApJ*, 202, 204
- Burbidge, E. M., Burbidge, G. R., Fowler, W. A., & Hoyle, F. 1957, *Rev. Mod. Phys.*, 29, 547
- Costa, V., Rayet, M., Zappalà, R. A., & Arnould, M. 2000, *A&A*, 358, L67
- Fuller, G. M. & Meyer, B. S. 1995, *ApJ*, 453, 792
- Hoffman, R. D., Woosley, S. E., Fuller, G. M., & Meyer, B. S. 1996, *ApJ*, 460, 478
- Howard, W. M., Meyer, B. S., & Woosley, S. E. 1991, *ApJ*, 373, L5
- Meyer, B. S. 1995, *ApJ*, 449, L55
- . 2002, *Physical Review Letters*, 89, 231101
- Qian, Y.-Z. & Woosley, S. E. 1996, *ApJ*, 471, 331
- Rauscher, T. & Thielemann, F. 2000, *Atom. Dat. Nucl. Dat. Tables*, 75, 1
- Schatz, H., Aprahamian, A., Barnard, V., Bildsten, L., Cumming, A., Ouellette, M., Rauscher, T., Thielemann, F.-K., & Wiescher, M. 2001, *Physical Review Letters*, 86, 3471
- Thompson, T. A., Burrows, A., & Meyer, B. S. 2001, *ApJ*, 562, 887
- Travaglio, C., Gallino, R., Arnone, E., Cowan, J., Jordan, F., & Sneden, C. 2004, *ApJ*, 601, 864
- Wallace, R. K. & Woosley, S. E. 1981, *ApJS*, 45, 389

Woosley, S. E. & Howard, W. M. 1978, ApJS, 36, 285

Woosley, S. E. & Weaver, T. A. 1995, ApJS, 101, 181

Yin, Q., Jacobsen, S. B., & Yamashita, K. 2002, Nature, 415, 881

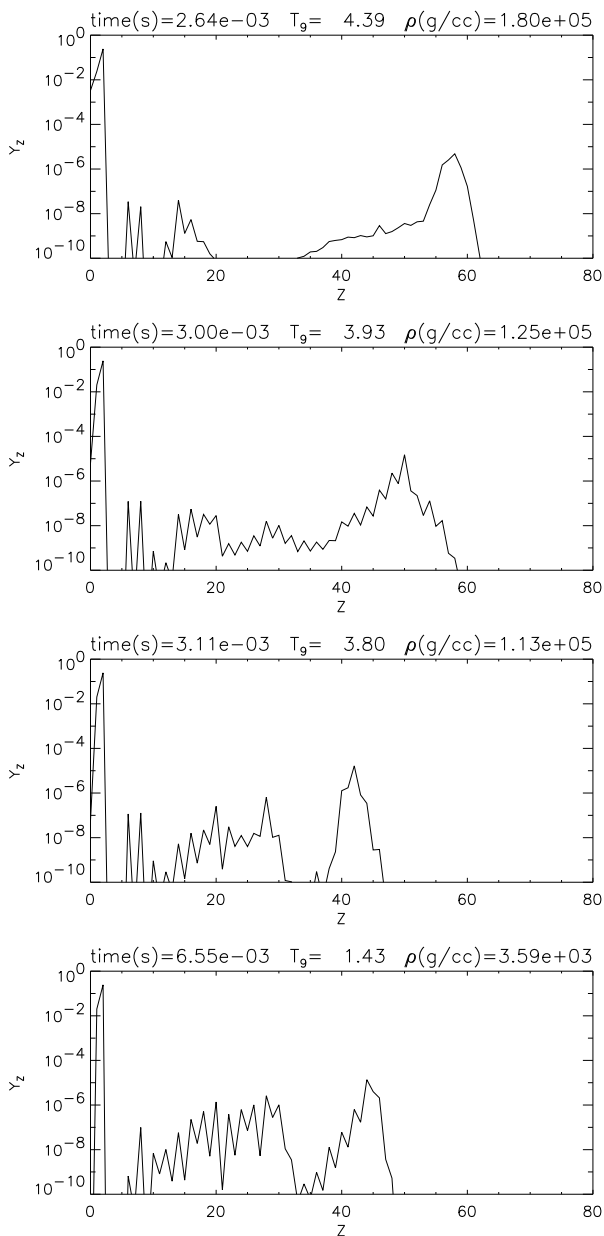


Fig. 1.— Elemental abundance versus mass number A for four times during the $\tau = 0.003$ s, $s = 145 k_B$, $Y_e = 0.510$ expansion.

Table 1. Ten most overproduced isotopes in calculations of fast, high-entropy, proton-rich expansions

rank	A ^a		B ^b		C ^c		D ^d		E ^e		F ^f	
	<i>AZ</i>	<i>O</i>	<i>AZ</i>	<i>O</i>	<i>AZ</i>	<i>O</i>	<i>AZ</i>	<i>O</i>	<i>AZ</i>	<i>O</i>	<i>AZ</i>	<i>O</i>
1	⁵⁹ Co	$5.31 \cdot 10^1$	⁹⁴ Mo	$2.15 \cdot 10^6$	¹¹² Sn	$7.91 \cdot 10^6$	¹⁸⁰ Ta	$7.71 \cdot 10^7$	²⁰¹ Hg	$7.91 \cdot 10^5$	⁵⁹ Co	$2.78 \cdot 10^2$
2	⁴⁵ Sc	$4.98 \cdot 10^1$	⁹⁶ Ru	$7.74 \cdot 10^5$	¹¹³ In	$3.88 \cdot 10^6$	¹⁸¹ Ta	$1.27 \cdot 10^6$	²⁰⁰ Hg	$5.34 \cdot 10^5$	⁶⁰ Ni	$3.95 \cdot 10^1$
3	⁶⁰ Ni	$4.25 \cdot 10^1$	⁹⁵ Mo	$3.87 \cdot 10^5$	¹⁰⁸ Cd	$2.09 \cdot 10^6$	¹⁷⁶ Lu	$7.70 \cdot 10^5$	²⁰⁴ Hg	$4.28 \cdot 10^5$	⁴⁵ Sc	$2.59 \cdot 10^1$
4	⁴⁹ Ti	$3.40 \cdot 10^1$	⁹² Mo	$5.40 \cdot 10^4$	¹¹⁰ Cd	$1.03 \cdot 10^6$	¹⁷⁵ Lu	$7.44 \cdot 10^5$	¹⁹⁹ Hg	$4.25 \cdot 10^5$	⁴⁹ Ti	$1.94 \cdot 10^1$
5	⁶³ Cu	$1.64 \cdot 10^1$	⁹³ Nb	$2.06 \cdot 10^4$	¹⁰⁶ Cd	$8.52 \cdot 10^5$	¹⁷⁴ Yb	$5.31 \cdot 10^5$	²⁰³ Tl	$3.25 \cdot 10^5$	⁶³ Cu	$1.84 \cdot 10^1$
6	⁴⁸ Ti	$1.31 \cdot 10^1$	⁸⁴ Sr	$1.22 \cdot 10^4$	¹²⁶ Xe	$4.86 \cdot 10^5$	¹⁷⁸ Hf	$5.23 \cdot 10^5$	²⁰² Hg	$3.18 \cdot 10^5$	⁴⁸ Ti	$1.46 \cdot 10^1$
7	⁴⁴ Ca	$1.09 \cdot 10^1$	⁹⁷ Mo	$1.17 \cdot 10^4$	¹¹⁴ Sn	$4.33 \cdot 10^5$	¹⁷¹ Yb	$5.22 \cdot 10^5$	¹⁹⁸ Pt	$1.94 \cdot 10^5$	⁴⁴ Ca	$1.17 \cdot 10^1$
8	⁴³ Ca	$8.28 \cdot 10^0$	⁹⁸ Ru	$6.47 \cdot 10^3$	¹¹⁵ Sn	$3.27 \cdot 10^5$	¹⁸² W	$4.15 \cdot 10^5$	¹⁸² W	$1.74 \cdot 10^5$	⁴³ Ca	$1.09 \cdot 10^1$
9	⁴⁷ Ti	$6.13 \cdot 10^0$	⁹¹ Zr	$4.39 \cdot 10^3$	¹²⁴ Xe	$1.59 \cdot 10^5$	¹⁸⁴ W	$3.61 \cdot 10^5$	¹⁸⁴ W	$1.61 \cdot 10^5$	⁴⁷ Ti	$6.41 \cdot 10^0$
10	⁵⁰ Cr	$6.11 \cdot 10^0$	⁹⁰ Zr	$2.37 \cdot 10^3$	¹⁰² Pd	$1.26 \cdot 10^5$	¹⁷⁶ Hf	$3.54 \cdot 10^5$	¹⁷⁹ Hf	$1.55 \cdot 10^5$	⁵¹ V	$6.08 \cdot 10^0$

^aCalculation A: $\tau = 0.003s$, $s=140$, initial $Y_e=0.510$

^bCalculation B: $\tau = 0.003s$, $s=145$, initial $Y_e=0.510$

^cCalculation C: $\tau = 0.003s$, $s=150$, initial $Y_e=0.510$

^dCalculation D: $\tau = 0.003s$, $s=160$, initial $Y_e=0.510$

^eCalculation E: $\tau = 0.003s$, $s=170$, initial $Y_e=0.510$

^fCalculation F: $\tau = 0.003s$, $s=145$, initial $Y_e=0.505$

Table 2. Ten most overproduced isotopes in calculations of with modified reaction rates.

rank	A ^a		B ^b	
	A_Z	O	A_Z	O
1	⁴⁵ Sc	$4.19 \cdot 10^1$	¹²⁶ Xe	$1.66 \cdot 10^7$
2	⁶⁰ Ni	$2.96 \cdot 10^1$	¹²⁴ Xe	$7.62 \cdot 10^6$
3	⁴⁹ Ti	$2.92 \cdot 10^1$	¹¹² Sn	$4.29 \cdot 10^6$
4	⁵⁹ Co	$1.38 \cdot 10^1$	¹³² Ba	$3.53 \cdot 10^6$
5	⁶³ Cu	$1.27 \cdot 10^1$	¹³⁰ Ba	$3.53 \cdot 10^6$
6	⁴⁸ Ti	$1.20 \cdot 10^1$	¹¹³ In	$2.44 \cdot 10^6$
7	⁴⁴ Ca	$9.89 \cdot 10^0$	¹³⁸ Ce	$1.96 \cdot 10^6$
8	⁴³ Ca	$7.42 \cdot 10^0$	¹²⁸ Xe	$1.15 \cdot 10^6$
9	⁴⁷ Ti	$5.41 \cdot 10^0$	¹¹⁴ Sn	$9.30 \cdot 10^5$
10	⁵⁰ Cr	$4.79 \cdot 10^0$	¹¹⁵ Sn	$9.07 \cdot 10^5$

^aCalculation A: $\tau = 0.003\text{s}$, $s=150$, initial $Y_e=0.510$; charged particle and EM rates for $Z \geq 27 \times 2$

^bCalculation B: $\tau = 0.003\text{s}$, $s=150$, initial $Y_e=0.510$; charged particle and EM rates for $Z \geq 27 \times 0.5$